PROMOTER MODIFICATIONS OF CATALYTIC ACTIVITY AND SELECTIVITY. PROGRESS REPORT, APRIL 1, 1982-NOVEMBER 30, 1983

COLORADO UNIV. AT BOULDER. DEPT. OF CHEMICAL ENGINEERING

30 NOV 1983

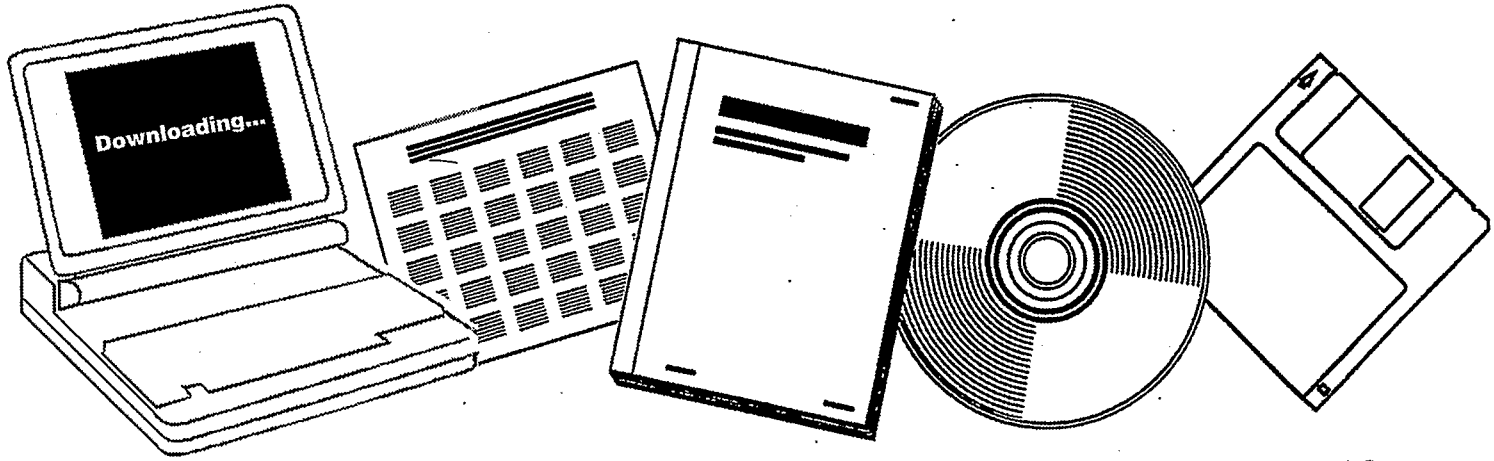

DE84003179

DOE/ER/12058--2

DE84 003179

"PROMOTER MODIFICATIONS OF CATALYTIC ACTIVITY AND SELECTIVITY"

Progress Report

for Period April 1, 1982-November 30, 1983

John L. Falconer
Associate Professor
Department of Chemical Engineering
University of Colorado, Campus Box 424
Boulder, Colorado 80309

November 30, 1983

Prepared for

The U.S. Department of Energy
Office of Basic Energy Sciences
Division of Chemical Sciences

Agreement #DE-AC02-82ER12058

NOTICE

Table of Contents

Abstract

The effect of alkali promoters on CO hydrogenation on supported nickel catalysts was studied as a function of catalyst support (Al_2O_3, SiO_2, $SiO_2 \cdot Al_2O_3$, and TiO_2), promoter concentration, catalyst preparation and alkali salt used in preparation. Activities, activation energies and product distributions of olefins and paraffins were measured over a range of temperatures in a differential reactor at steady state. On all catalysts except $Ni/SiO_2 \cdot Al_2O_3$, the activity decreased with promoter addition though the decrease was very large for Ni/TiO_2 and very small for Ni/Al_2O_3. On Ni/SiO_2, the rate of hydrogenation was studied as a function of concentration and a rapid decrease was seen with increased potassium concentration. The influence of promoter salt and preparation method were found to be small relative to the effect of support or promoter concentration. The oxide support significantly changed alkali promotion. On $Ni/SiO_2 \cdot Al_2O_3$, the rates of formation for all paraffins went through a maximum and then slowly decreased with promoter concentration. Selectivities to olefins increased dramatically on most promoted catalysts (except $Ni/SiO_2 \cdot Al_2O_3$), though this was usually at the expense of paraffin formation.

Temperature-programmed reaction (TPR) on many of these catalysts showed excellent agreement with differential reactor studies. Rates of methane and ethane formation decreased on Ni/SiO_2 and Ni/TiO_2 but they increased on $Ni/SiO_2 \cdot Al_2O_3$. These TPR studies also showed that changes in rate were not due to site blocking. Carbon hydrogenation was also observed to decrease with promotion and temperature-programmed desorption indicated decreased hydrogenation rates for carbon monoxide, carbon and olefins was due to weakened hydrogen bonding. Carbon monoxide desorption also was observed to change significantly with promotion.

Research Scope and Objectives

The influence of alkali promoters on catalytic activity and selectivity for carbon monoxide hydrogenation is being studied on supported metal catalysts. The interaction of the promoter and the oxide support, and the effect of promoter concentration and preparation method are of interest. Temperature-programmed desorption (TPD) and reaction (TPR) are used with mass spectrometric detection to determine how promoters affect binding energies, individual reaction steps, reaction mechanism and specific activity. Selectivity and activity are measured in a differential reactor with gas chromatographic analysis. The aim of this research is to understand how a catalytically-inert alkali metal modifies CO hydrogenation and to determine if the changes in activity and selectivity due to the promoter are affected by the support.

Project Status, Accomplishments and Technical Discussion

Temperature-programmed desorption (TPD) and reaction (TPR) and differential reactor studies were used to study CO hydrogenation on supported nickel catalysts. Four supports (SiO_2, Al_2O_3, TiO_2 and $SiO_2 \cdot Al_2O_3$) were used to prepare catalysts by impregnation. Sodium was added by preimpregnation of NaCl and by coimpregnation of $NaNO_3$. Potassium was added by pre-, co- and post-impregnation using KCl, $K_2C_2O_4$, K_2CO_3 and KOH. On Ni/SiO_2 and $Ni/SiO_2 \cdot Al_2O_3$, the concentration of potassium was also varied.

The changes in the activity and selectivity were studied in a differential reactor for a 3:1 H_2:CO mixture at atmospheric pressure. Alkali promoters were found to have a very large effect on both the activity and selectivity to higher hydrocarbons. However, the support significantly influenced these changes in kinetic properties. The method of promoter addition had smaller effects on activity and selectivity.

Both nickel and alkali metal weight loadings were measured by atomic absorption since the activity was found to be very sensitive to alkali

concentration. Some of the catalysts were also characterized by Auger spectroscopy and x-ray photoelectron spectroscopy to verify the presence of alkali.

Differential Reactor Studies

A differential reactor system with sand bath heater and gas chromatograph detection was designed and constructed. Rates, selectivities to higher hydrocarbons and activation energies were measured in agreement with those reported in the literature. Catalytic activities and selectivities were then compared for catalysts on various supports, with and without promoters. Data are for a 3:1 ratio of H_2:CO and for conversions below five percent.

For most catalysts, methane and paraffin activities decreased with potassium addition. Olefin activity decreased much slower or it increased, so that the selectivity to C_2 to C_4 olefins increased dramatically. For 1% K on 10% Ni catalysts, the methane activity decreased a factor of 70 for SiO_2 support and a factor of 45 for a TiO_2 support. The methane activity decreased only a factor of 3 on Al_2O_3 and the activity increased slightly for a $SiO_2 \cdot Al_2O_3$ support. On $Ni/SiO_2 \cdot Al_2O_3$, methane and paraffin activities go through a maximum with promoter concentration.

Alkali promoters increased olefin selectivity and the olefin to paraffin ratio significantly. The ratio of olefin to paraffin formation increased a factor of 200 on Ni/SiO_2 for C_2 and 100 for C_3. The support did not change the olefin selectivity much, but the promoter did. The promoter effect is in addition to the support effect. Thus, on promoted Ni/TiO_2, more than 50% of the product were olefins. Figures 1 and 2 show the hydrocarbon product selectivities at three temperatures for unpromoted and potassium-promoted Ni/TiO_2. Because of the large differences in activities, comparisons at the same temperature are difficult.

Table 1 presents the activities and activation energies for 10% Ni on the four supports. As can be seen, there is a large dependence on support.

Detailed studies for various preparation methods, promoter salts and promoter concentrations were completed for Ni/SiO_2 catalysts. Figure 3 shows that for Ni/SiO_2 catalysts, the methanation activity decreased very rapidly with potassium concentration. Similarly, the activities for C_2-C_4 paraffins decreased rapidly while olefin activities remained constant or increased. Thus, olefin selectivity increased dramatically. This is shown in Figure 4. For example, for 0.74% K, methane activity decreased a factor of 22 while ethylene activity increased a factor of 10. As noted in Table 1, the change in activation energy was not large, with few exceptions.

Tables 2 and 3 show that using different potassium salts had little influence on catalytic activity; the main influence was due to the amount of potassium present. Similarly, the method of preparation appeared to have a small influence on the activity or selectivity. There are some indications that higher activities are obtained for certain methods of preparation but this is still being studied. In general, a good correlation was found between inverse activity and olefin/paraffin ratio, as shown in Figure 5. This plot was made for two supports, four promoter salts, four methods of preparation and a range of concentrations. High olefin yields were only obtained at lower overall activities. Also, the olefin/paraffin ratio was significantly higher for C_3 than for C_2 hydrocarbons for all catalysts.

Tables 4 and 5 and Figure 6 show that $Ni/SiO_2 \cdot Al_2O_3$ catalysts exhibited a distinct maximum in both methane activity and total activity with promoter concentration. However, the olefin selectivity did not increase dramatically on $Ni/SiO_2 \cdot Al_2O_3$, even at the higher concentrations of K. At low potassium loadings, the olefin selectivities decreased with potassium addition. Figure 7 shows the product distributions. The rapid decrease in activity with promoter concentration that was observed for Ni/SiO_2 was not seen for $Ni/SiO_2 \cdot Al_2O_3$.

Note that activities versus promoter concentration are plotted on a linear scale for $Ni/SiO_2 \cdot Al_2O_3$ while the activities for Ni/SiO_2 were on a log scale. Thus, the effect of potassium is very different on Ni/SiO_2 and $Ni/SiO_2 \cdot Al_2O_3$.

The methane activation energies for $Ni/SiO_2 \cdot Al_2O_3$ catalysts were very similar; all values were equal to 114 ± 6 kJ/mol. Also, KCl and K_2CO_3 promoters gave similar activities for similar concentrations of potassium.

Temperature-Programmed Reaction

Temperature-programmed reaction for CO hydrogenation showed that the decreased methane activities seen in steady-state kinetic measurements were not due to site blocking or to decreased dispersion; the specific rates of reaction decreased. Agreement between TPR and differential reactor studies was very good. On $Ni/SiO_2 \cdot Al_2O_3$, the specific rate of methanation increased while on the other catalysts, the rate decreased. This excellent agreement between TPR and steady-state kinetic studies shows that TPR can be used as a rapid method of characterizing reaction properties of supported catalysts. Table 6 shows the peak temperatures for some of the catalysts on which TPR was run. Note that not only methane but higher paraffin rates are also decreased as promoters are added. This is in agreement with the steady-state kinetic studies. Figure 8 shows the significant change in activity as promoters are added. Note that only a small amount of ethane is formed and that both methane and ethane rates are decreased by promoter addition.

Carbon was deposited by CO disproportionation at 573 K and the rate of carbon hydrogenation was studied by temperature-programmed reaction. On Ni/SiO_2 both sodium and potassium decreased the rate of carbon hydrogenation, apparently due to the decreased hydrogen bonding.

Ni/TiO_2: The hydrogenation of CO on 10% Ni/TiO_2 was studied in detail using TPR since Ni/TiO_2 has a high selectivity to higher hydrocarbons and the

selectivity is further increased by the addition of alkali promoters. Both the effect of reduction temperature and the effect of initial coverage were studied.

The initial coverage was varied by interrupted reaction. After CO adsorption to saturation coverage, the catalyst was heated in hydrogen to a specified temperature, cooled to room temperature and then heated at 1 K/s to 723 K in a normal TPR. Using computer switching between mass peaks, methane (mass 15), ethane (mass 30), propane (mass 43) and mass 44 (propane and carbon dioxide) were simultaneously monitored as a function of temperature. Figures 9 and 10 show the methane and ethane products for seven different initial coverages.

Methane and ethane were formed in narrow peaks and two distinct methane peaks were seen. Ethane formed at a slightly lower temperature than methane; the ethane yield was only one-hundredth of the methane. The methane, ethane and propane peak temperatures did not change with initial coverage, indicating first-order processes for all three products. Masses 43 and 44 were used to identify propane. Since mass 44 was broader than 43, it probably has a contribution from CO_2 and from propane. Olefins are not expected to form in TPR experiments because of the large excess of H_2. Also, ethylene would be difficult to detect because of desorption of unreacted CO.

Even for the high H_2:CO ratio that is present during TPR, the Ni/TiO_2 catalyst still forms ethane and propane. Though these quantities are small, they are detectable with the mass spectrometer system, and so the results show the sensitivity of TPR for studying catalytic reactions.

Promoted Ni/TiO_2: As mentioned, adding potassium to Ni/TiO_2 caused a significant decrease in the rate of reaction, as seen in steady state. Temperature-programmed reaction also observed a large increase in methane and ethane peak temperatures, as well as an increase in the temperature of unreacted CO. Figure 11 shows the methane peaks and the unreacted CO. A larger fraction of the adsorbed CO was observed desorbing for the promoted Ni/TiO_2.

Ni/Al_2O_3: An extensive temperature-programmed reaction study of low-weight loading nickel/alumina catalysts was completed. These Ni/Al_2O_3 catalysts showed a strong support effect and they also demonstrated the presence of mutliple reaction sites for methane. Two distinct pathways, corresponding to two distinct sites for CO adsorption, are present for CO hydrogenation to methane. Figure 12 shows the two CH_4 peaks and the unreacted CO. The activation energies were measured for each site and conversion between sites was observed to be influenced by hydrogen. The high-temperature site was also found to be sensitive to the pretreatment temperature. Neither of the sites was found to be limited by carbon hydrogenation. Carbon was deposited by CO disproportionation and the subsequent hydrogenation in TPSR is shown in Figure 13. This study demonstrates the ability of temperature-programmed reaction to measure specific reaction rates and to separate reaction pathways that might be obscured in steady-state kinetic measurements.

The presence of two sites was attributed to the interaction of alumina with the supported nickel. One site corresponds to CO adsorbed on nickel atoms that are interacting with other nickel atoms. The second site results from CO adsorbed on nickel atoms interacting with an oxide phase. The first site had a methanation activation energy of 51 kJ/mol and the second had an energy of 145 kJ/mol.

The effect of promoters on low weight loading Ni/Al_2O_3 will be studied with particular emphasis on determining which site is affected at low promoter concentrations.

Temperature-Programmed Desorption

Hydrogen desorption in He, following saturation adsorption of hydrogen, was studied by temperature-programmed desorption (TPD). As shown in Figure 14a, hydrogen desorbed from Ni/SiO_2 over a broad temperature range. This broad peak has been attributed to readsorption of the hydrogen. When alkali promoter

was added to Ni/SiO_2, hydrogen bonding decreased significantly; one example of this is shown in Figure 14b. When 0.9% K potassium was added to 12% Ni/SiO_2, the peak temperature decreased and the temperature at which desorption was complete also decreased.

Similarly, on Ni/TiO_2, hydrogen desorbed from the unpromoted catalyst over a wide temperature range (Figure 15). Addition of potassium also weakened the hydrogen bonding to the surface. Hydrogen adsorption also appeared to be activated.

These changes in hydrogen bonding appear to be reflected in the TPR and steady-state experiments. Since promoters weaken hydrogen bonding on Ni/TiO_2 and Ni/SiO_2, the rates of CO and C hydrogenation decrease in TPR. Similarly, the rates of hydrogenation of CO to methane and higher paraffins also decrease. Thus, more olefins are observed on the promoted catalysts. Consistent with this is the observation that hydrogen bonding on $Ni/SiO_2 \cdot Al_2O_3$ is increased slightly with the addition of promoters. This is something that we need to study in more detail.

Carbon monoxide bonding was also significantly changed on promoted Ni/TiO_2. Figure 16 shows CO desorption from Ni/TiO_2 for a series of interrupted TPD. Note that some CO desorbs at low temperatures and is very weakly bound. Also present is CO that is very strongly bound to the surface and its desorption is not complete by 700 K. When 1% K was added, however, the strongly-bound and the weakly-bound CO are almost eliminated. The remaining CO in the 500-600 K range is more strongly bound than on the unpromoted Ni/TiO_2 (see Figure 17).

Temperature-programmed desorption of CO also yields CO_2 due to disproportionation. On unpromoted Ni/TiO_2, the CO_2 is observed over a relatively narrow temperature range (Figure 18). After addition of promoter, the amount of CO_2 is decreased drastically and the CO_2 also forms at a lower temperature (Figure 19). Relating these changes in CO bonding and disproportionation to changes in activity is difficult and further experiments are in progress to do this.

Conclusions

Carbon monoxide hydrogenation to methane and higher hydrocarbons was changed significantly by the addition of alkali promoters to supported nickel catalysts. Alkali promoters in general were observed to decrease activity and increase olefin selectivity. However, the oxide support significantly affects the modifications induced by the promoters. On SiO_2, Al_2O_3 and TiO_2, overall activity decreased; on $SiO_2 \cdot Al_2O_3$, activity increased with promoters and a maximum was observed at low potassium concentrations. Differential reactor studies were also used to show that the support and promoter concentrations had a larger influence on activity and selectivity than catalyst preparation (pre-, co- or postimpregnation) and promoter salt used (KCl, K_2CO_3, $K_2C_2O_4$, KOH).

Temperature-programmed reaction (TPR) also showed that alkali decreased the rates of both carbon monxoide and carbon hydrogen; the decreased rates were not due to site blocking. Excellent agreement was obtained between TPR and steady-state kinetics. Temperature-programmed desorption (TPD) indicated that the decreased hydrogenation rates of CO, carbon and of olefin were due to weakened hydrogen bonding. The CO desorption was also significantly changed by promotion.

Table 1

Activity at 548 K and Activation Energies

Catalyst*	CH_4 Activity (μmol/g·Ni·S)	E_{CH_4} (kJ/mol)	Total Activity (μmol/g·Ni·S)	E_{CO} (kJ/mol)
16% Ni/SiO_2	83	103	110	82
11% Ni/0.8% K/SiO_2	1.2	146	1.9	149
8.9% Ni/0.7% K/SiO_2	3.3	128	6.9	113
9.6% Ni/Al_2O_3	120	128	220	112
10% Ni/0.8% K/Al_2O_3	35	119	84	100
9.4% $Ni/SiO_2 \cdot Al_2O_3$	110	110	130	77
9.7% Ni/0.8% $K/SiO_2 \cdot Al_2O_3$	110	125	150	96
9.7% Ni/TiO_2 (450°C)	260	129	670	105
10% Ni/0.8% K/TiO_2 (450°C)	4.7	125	14	99
9.7% Ni/TiO_2 (500°C)	220	133	560	105
10% Ni/0.8% K/TiO_2 (500°C)	4.6	122	14	96
9.7% Ni/TiO_2 (550°C)	170	136	420	106

*Reduction temperature indicated for TiO_2 catalysts. All other catalysts reduced at 500°C.

Table 2

Ni/SiO_2 Catalysts

#	% Ni	% K	Preparation Method	Promoter Salt
1	9.2	0.0	Impregnation	Unpromoted
2	11.0	0.25	Pre-impregnation(A) II	K_2CO_3
3	9.2	0.68	Co-impregnation(B) IV	$K_2C_2O_4$
4	9.2	0.70	Co-impregnation(B) IV	$K_2C_2O_4$
5	8.9	0.74	Co-impregnation(B) IV	$K_2C_2O_4$
6	9.2	0.80	Calcination(D) V	$K_2C_2O_4$
7	11.0	0.81	Pre-impregnation(A) II	KCl
8	9.8	0.89	Calcination(D) V	KOH
9	9.2	0.90	Post-impregnation(C) III	KOH

Table 3

Ni/SiO_2 Catalysts

#	Catalyst(%K)	CH_4 Activity (μmol/g·Ni·S)	E_{CH_4} (kJ/mol)	Total Activity (μmol/g·Ni·S)	C_2H_4 Activity (μmol/g·Ni·S)
1	0.0	145	122	182	0.06
2	0.25	47	94	67	0.13
3	0.68	5.1	131	10.3	0.74
4	0.70	3.6	138	7.3	0.58
5	0.74	4.0	128	8.5	0.68
6	0.80	2.5	136	5.9	0.67
7	0.81	2.2	126	4.1	0.43
8	0.89	1.5	141	3.5	0.46
9	0.90	14.5	121	23.8	0.61

Table 4

$Ni/SiO_2 \cdot Al_2O_3$ Catalysts

#	% Ni	% K	Preparation Method	Promoter Salt
15	9.5	0.0	Impregnation	Unpromoted
16	11.5	0.25	Pre-impregnation(A) II	K_2CO_3
17	12	0.43	Pre-impregnation(A) II	K_2CO_3
18	9.7	0.81	Pre-impregnation(A) II	KCl
19	11.0	0.93	Pre-impregnation(A) II	K_2CO_3
20	11.0	0.97	Calcination(D) V	K_2CO_3
21	11.0	2.0	Calcination(D) V	K_2CO_3
22	11.5	3.9	Pre-impregnation(A) II	K_2CO_3

Table 5

$Ni/SiO_2 \cdot Al_2O_3$ Catalysts

#	Catalyst(%K)	CH_4 Activity (μmol/g·Ni·S)	E_{CH_4} (kJ/mol)	Total Activity (μmol/g·Ni·S)	C_2H_4 Activity (μmol/g/·Ni·S)
15	0.0	116	110	140	0.08
16	0.25	222	107	278	0.06
17	0.43	187	115	244	0.07
18	0.81	117	125	151	0.11
19	0.93	134	119	183	0.09
20	0.97	112	113	160	0.20
21	2.0	23	109	37	0.61
22	3.9	18	116	31	0.39

Table 6

Peak Temperatures (K) from TPR of Carbon Monoxide

Catalyst	CH_4	C_2H_6	C_3H_8
Ni/SiO_2			
unpromoted	484	461	484
0.5% Na*	493	472	475
0.5% Na	514	500	497
0.6% K	521	488	497
0.9% K	550	498	447
$Ni/SiO_2 \cdot Al_2O_3$			
unpromoted	471	444	--
0.2% Na	465	445	442
0.3% Na	460,519	432	455

Figure Captions

Figure 1 Product distribution on unpromoted 10% Ni/TiO at three temperatures.

Figure 2 Product distribution on 10% Ni/TiO_2 promoted with 1% K. Because of the reduced activity, the distributions are shown at higher temperatures than in Figure 1.

Figure 3 Log of CO conversion activity versus potassium concentration for potassium-promoted Ni/SiO_2 catalysts. The different symbols correspond to different methods of preparation and different promoter salts.

Figure 4 Hydrocarbon product distributions for three Ni/SiO_2 catalysts.

Figure 5 Relation between olefin to paraffin ratio and inverse activity for potassium-promoted Ni/SiO_2 (closed circles) and $Ni/SiO_2 \cdot Al_2O_3$ (open circles). The different symbols correspond to different methods of preparation and different promoter salts.

Figure 6 CO conversion activity versus potassium concentration on promoted $Ni/SiO_2 \cdot Al_2O_3$ catalysts.

Figure 7 Hydrocarbon product distributions for unpromoted $Ni/SiO_2 \cdot Al_2O_3$ and for promoted $Ni/SiO_2 \cdot Al_2O_3$ catalysts.

Figure 8 Hydrocarbon products for TPR of CO from Ni/SiO_2 (a) CH_4 (b) C_2H_6 and from 0.9% K on Ni/SiO_2 (c) CH_4 (d) C_2H_6.

Figure 9 Methane TPR spectra for CO adsorbed on 10% Ni/TiO_2. Initial coverage was varied by interrupted reaction.

Figure 10 Ethane TPR spectra for CO adsorbed on 10% Ni/TiO_2. Initial coverage was varied by interrupted reaction.

Figure 11 Methane and unreacted CO for TPR of CO on unpromoted and promoted Ni/TiO_2.

Figure 12 Methane TPR spectra and unreacted CO from a 4.7% Ni/Al_2O_3 catalyst.

Figure 13 Methane formed from hydrogenation of carbon deposited on 4.7% Ni/Al_2O_3.

Figure 14 Hydrogen desorption spectra for hydrogen adsorption at 298 K on (a) 10.1% Ni/SiO_2 (b) 12.1% Ni/SiO_2 with 0.9% K promoter.

Figure 15 Hydrogen desorption from unpromoted Ni/TiO_2. Adsorption was done in flowing hydrogen as the catalyst was cooled from 700 K.

Figure 16 Carbon monoxide desorption from Ni/TiO_2. Initial coverage was varied by interrupted desorption.

Figure 17 Carbon monoxide desorption from 0.9% K promoted Ni/TiO_2.

Figure 18 Carbon dioxide formation following CO adsorption on Ni/TiO_2.

Figure 19 Carbon dioxide formation following CO adsorption on potassium-promoted Ni/TiO_2.

10% Ni/TiO2 (without Promoter)
= unsaturated
- saturated
Number of Carbons
Product Weight %
0
20
40
60
80
533 K
508 K
478 K
1 2= 2- 3= 3- 4 5+

Figure 1

10% Ni/1% K/TiO2 (with promoter)
= unsaturated
- saturated
Product Weight %
0
20
40
60
80
1 2= 2- 3= 3- 4 5+
624K
609K
560K
Number of Carbons

Figure 2

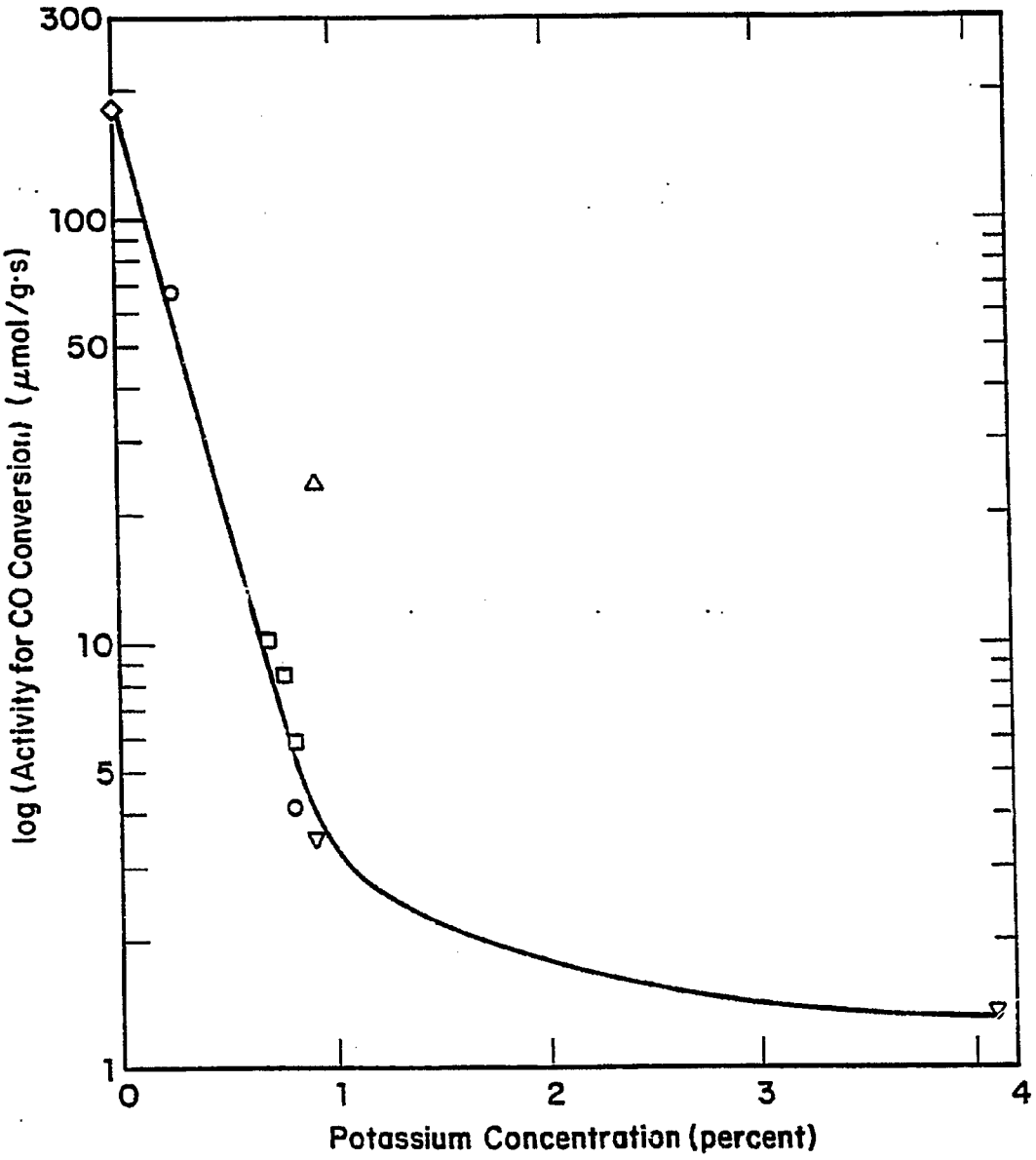
300
100
50
10
5
1
log (Activity for CO Conversion) (μmol/g·s)
0
1
2
3
4
Potassium Concentration (percent)

Figure 3

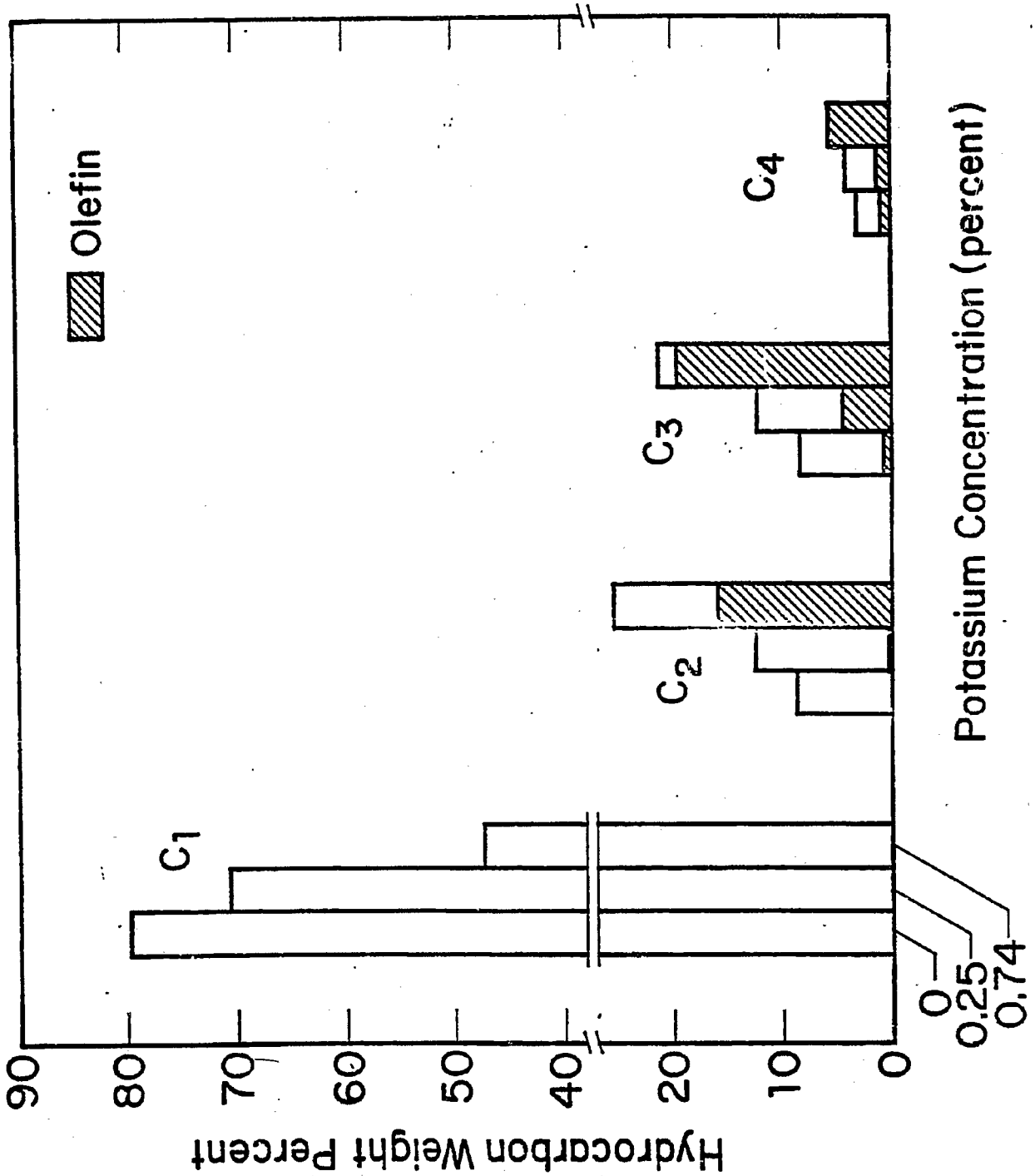
Hydrocarbon Weight Percent
90
80
70
60
50
40
20
10
0
Olefin
C1
C2
C3
C4
Potassium Concentration (percent)
0
0.25
0.74

Figure 4

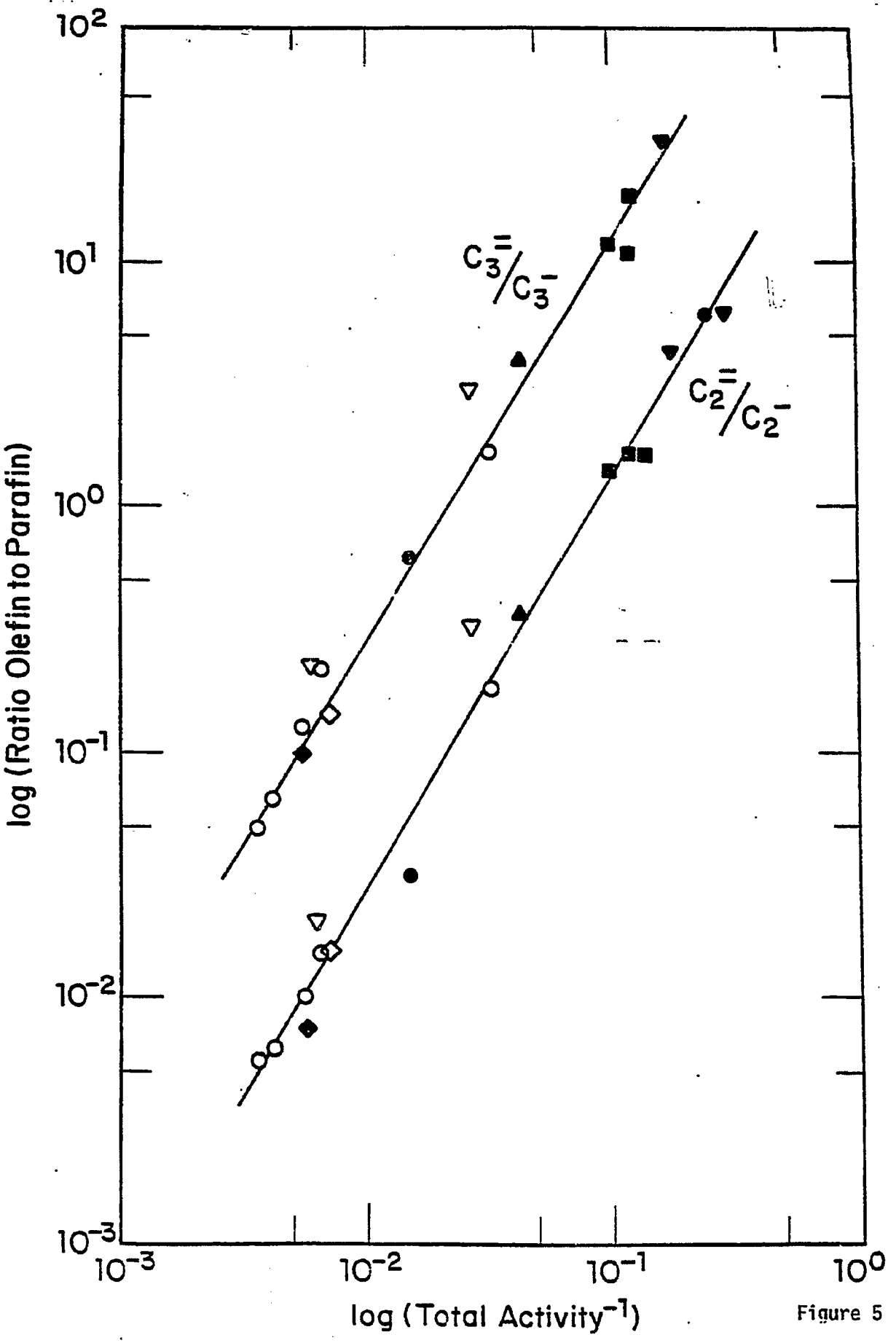
10^2
10^1
10^0
10^{-1}
10^{-2}
10^{-3}
10^{-3}
10^{-2}
10^{-1}
10^0
log (Ratio Olefin to Parafin)
log (Total Activity^{-1})
$C_3^=/C_3^-$
$C_2^=/C_2^-$

Figure 5

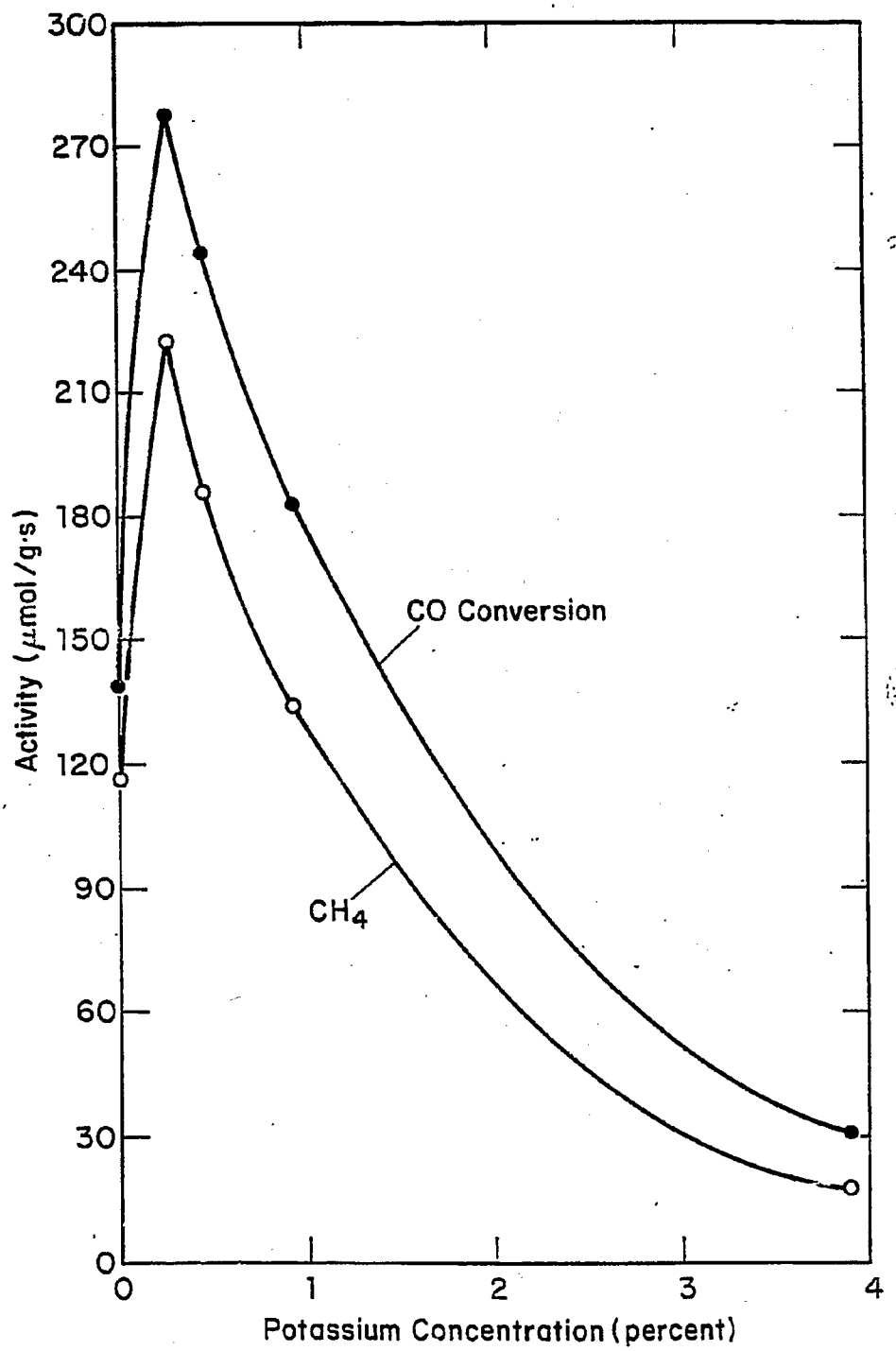
300
270
240
210
180
150
120
90
60
30
0
Activity (μmol/g·s)
CO Conversion
CH4
0
1
2
3
4
Potassium Concentration (percent)

Figure 6

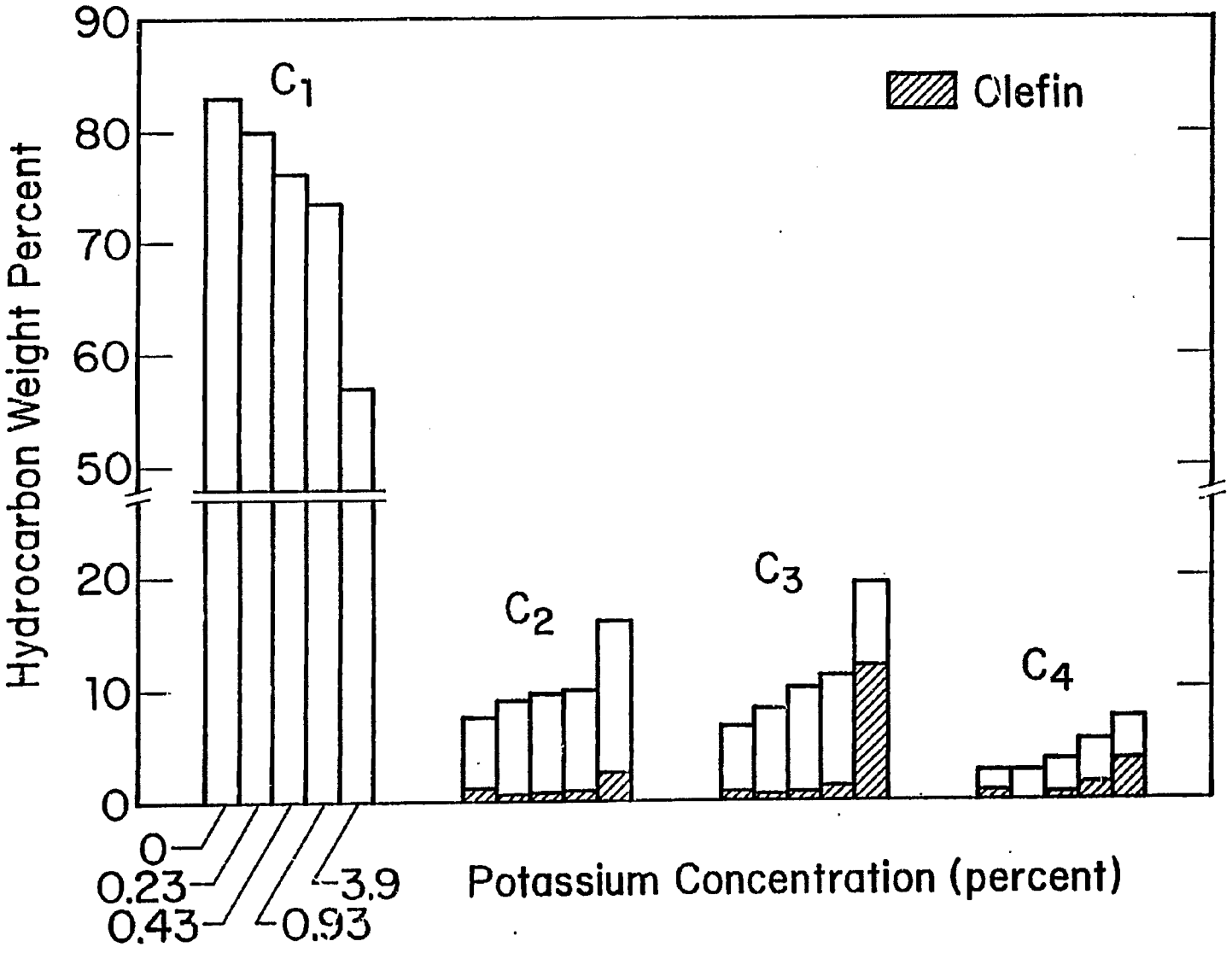
Hydrocarbon Weight Percent
90
80
70
60
50
20
10
0
C1
C2
C3
C4
Olefin
0
0.23
0.43
0.93
3.9
Potassium Concentration (percent)

Figure 7

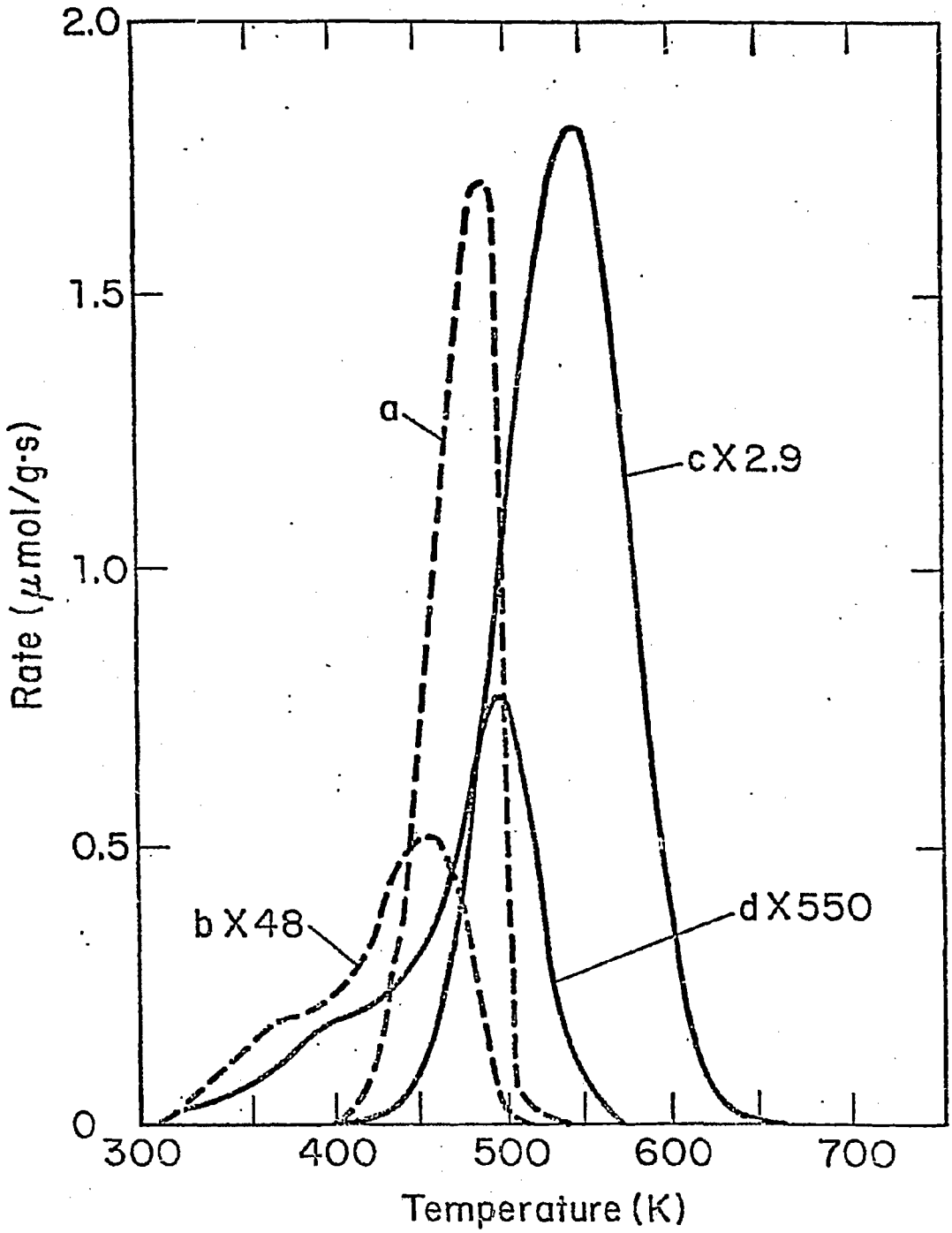
2.0
1.5
1.0
0.5
0
Rate (μmol/g·s)
a
b X48
c X2.9
d X550
300
400
500
600
700
Temperature (K)

Figure 8

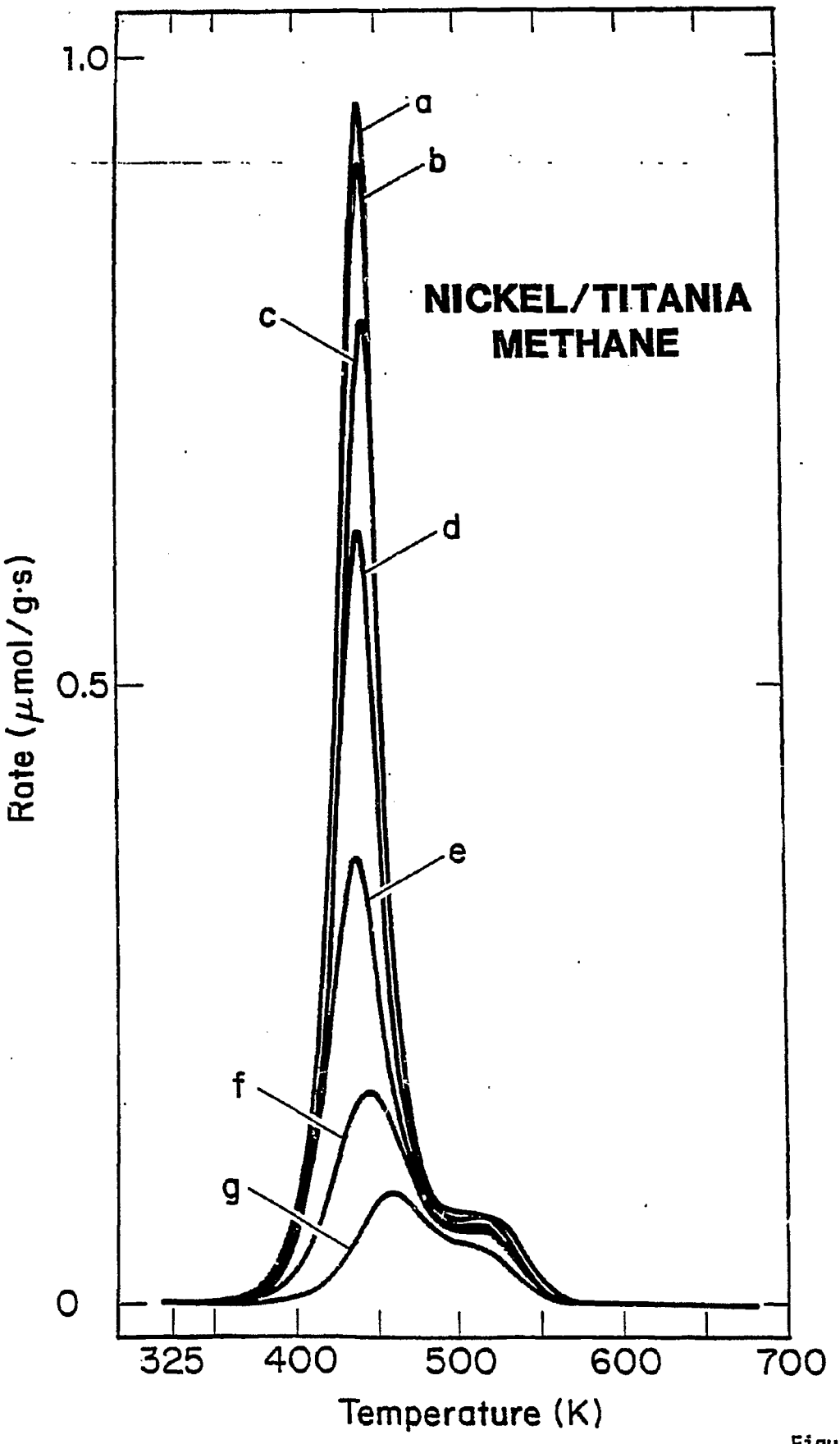
1.0
0.5
0
Rate (μmol/g·s)
a
b
c
d
e
f
g
NICKEL/TITANIA
METHANE
325
400
500
600
700
Temperature (K)

Figure 9

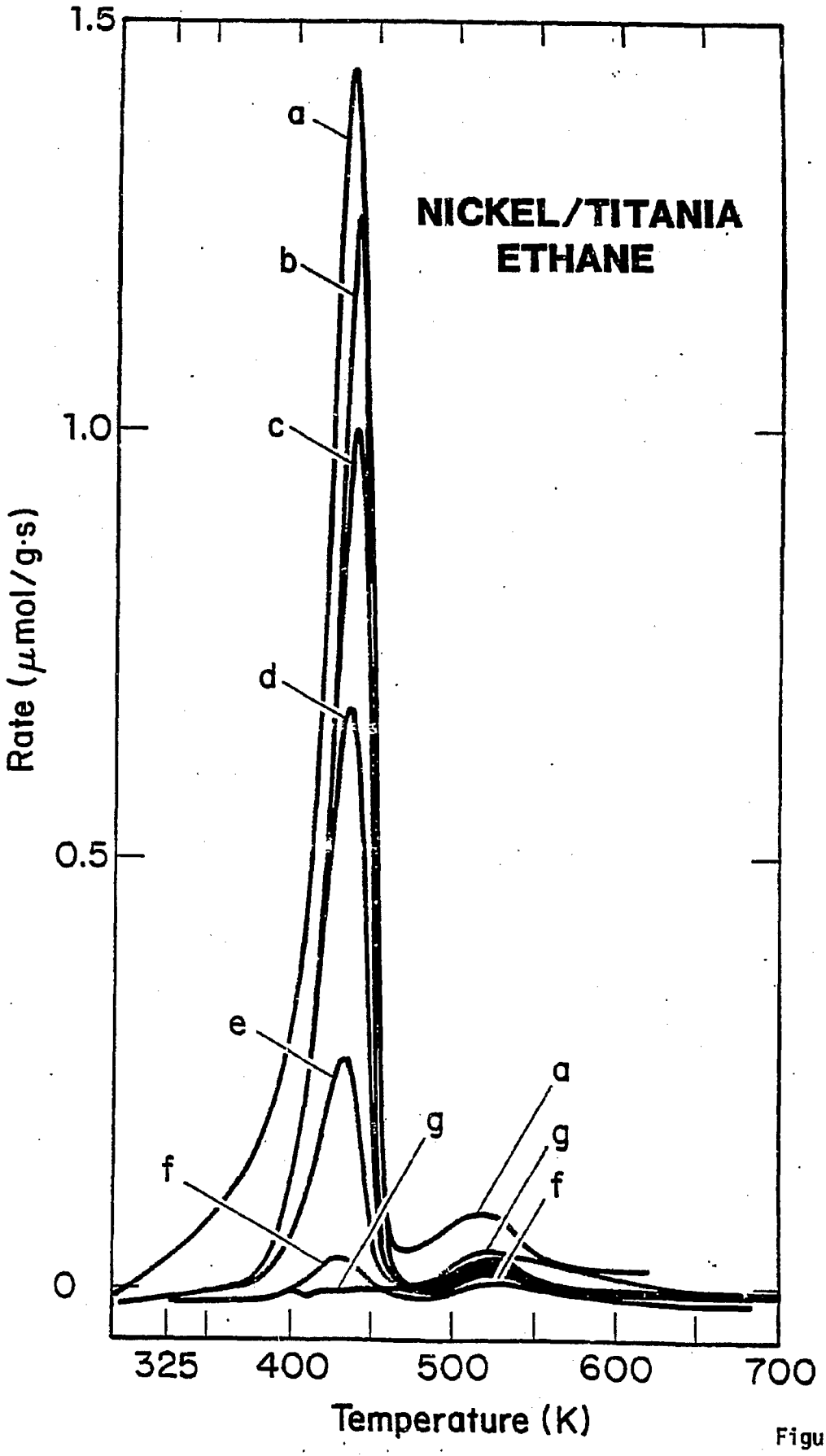
NICKEL/TITANIA
ETHANE
Rate (μmol/g·s)
1.5
1.0
0.5
0
325
400
500
600
700
Temperature (K)
a
b
c
d
e
f
g
a
g
f

Figure 10

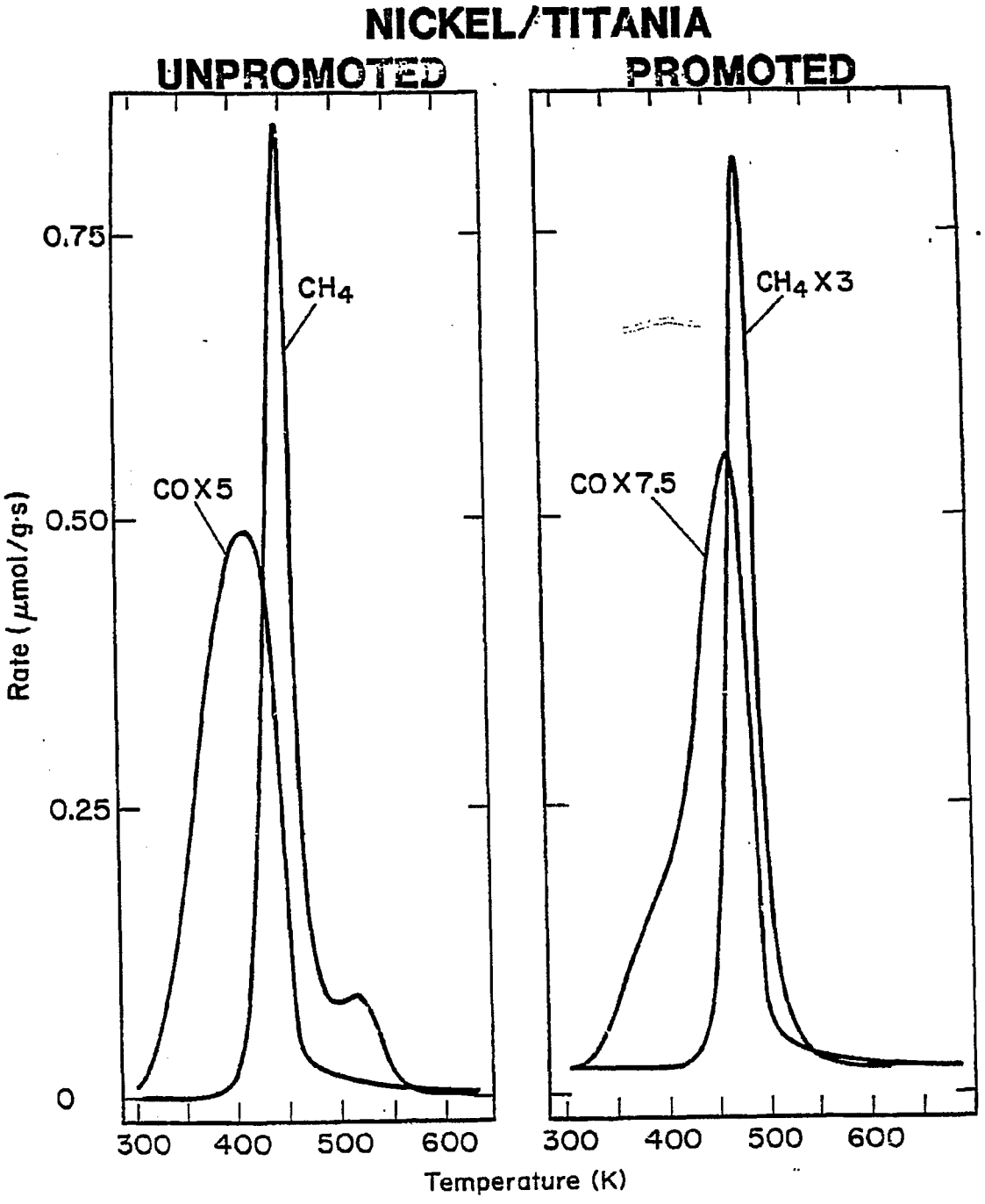
NICKEL/TITANIA
UNPROMOTED
PROMOTED
0.75
0.50
0.25
0
Rate (μmol/g·s)
CH4
CO X5
CH4 X3
CO X7.5
300
400
500
600
Temperature (K)

Figure 11

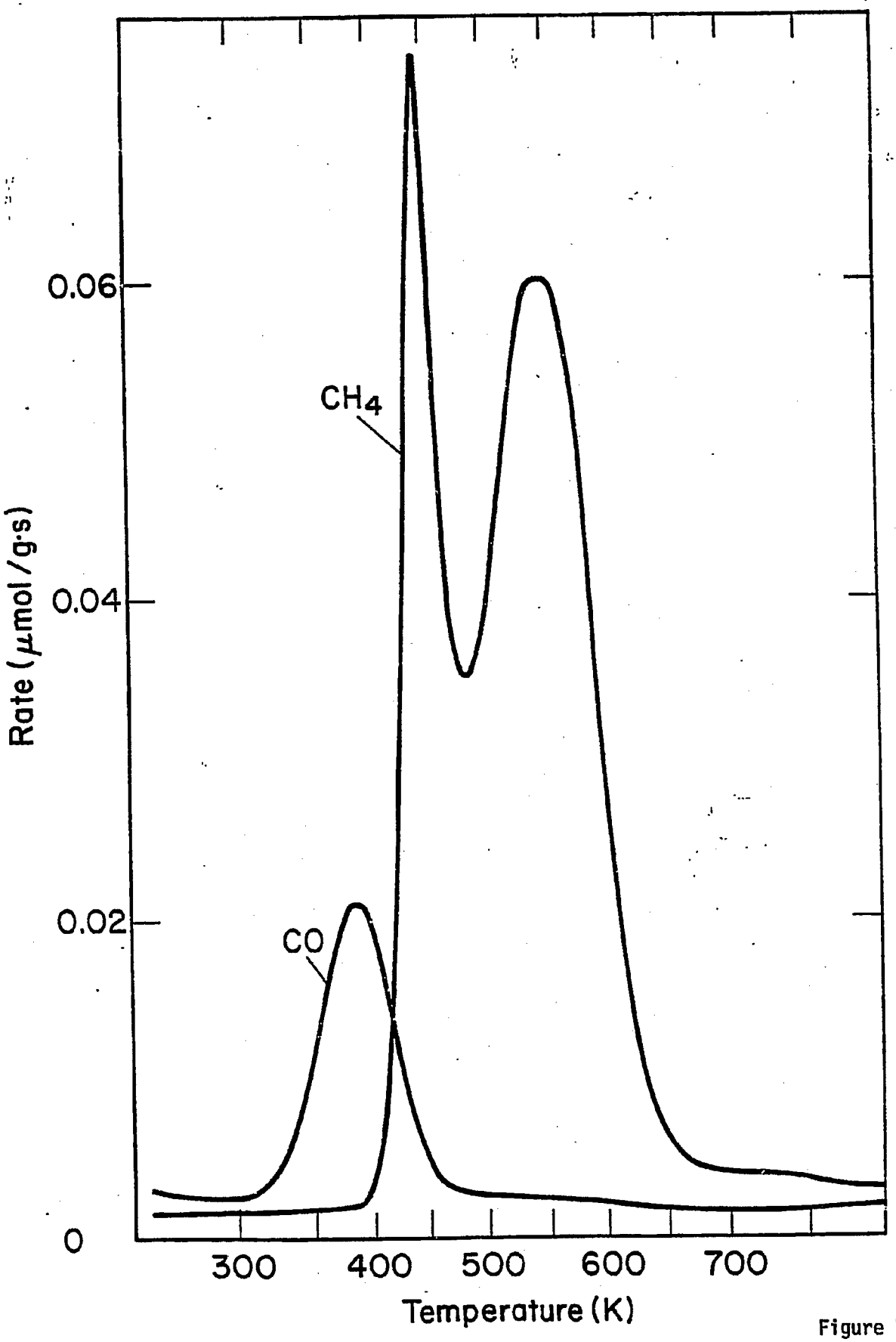
0.06
0.04
0.02
0
Rate (μmol/g·s)
CH4
CO
300
400
500
600
700
Temperature (K)

Figure 12

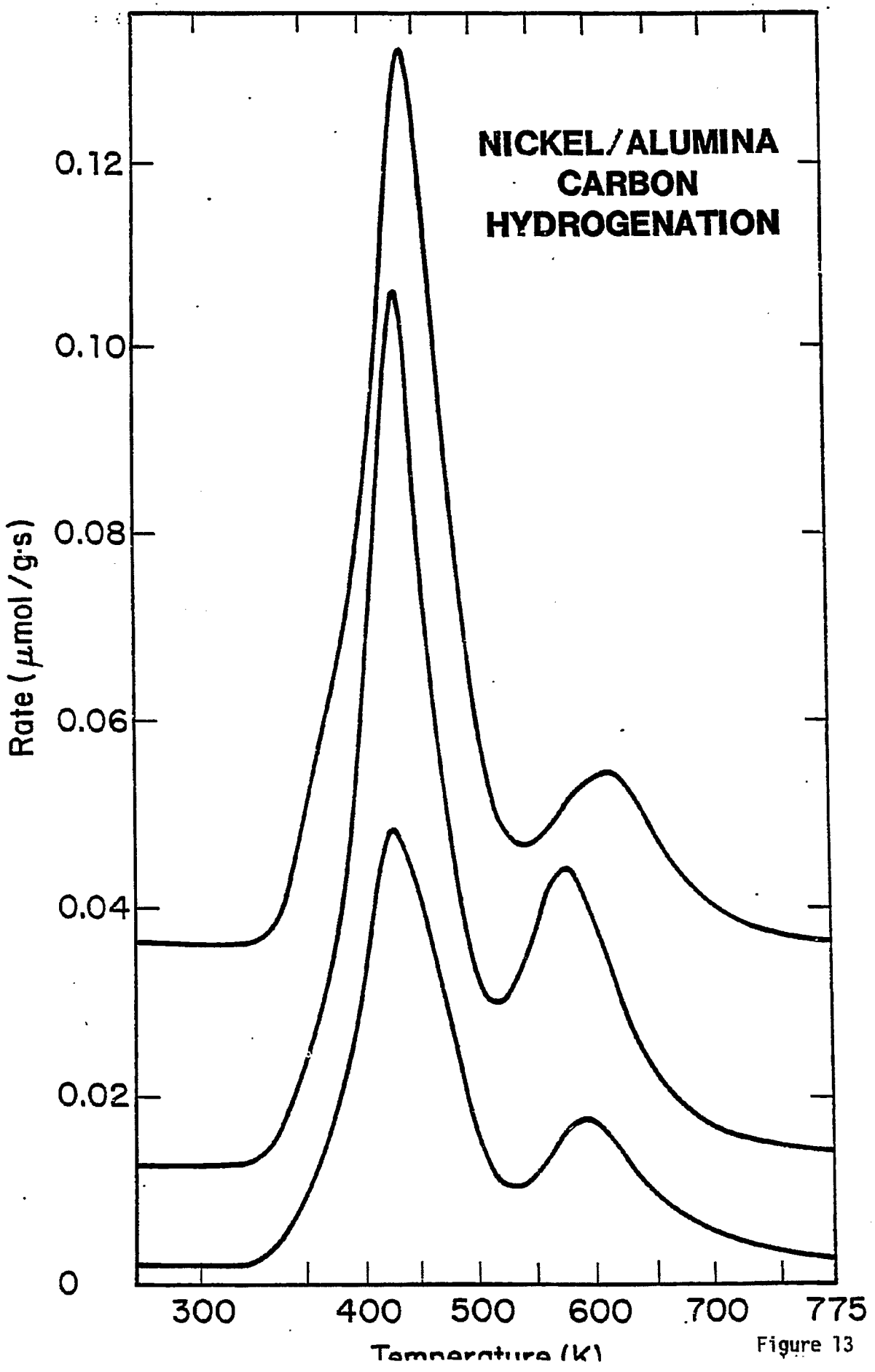
NICKEL/ALUMINA
CARBON
HYDROGENATION
Rate (μmol/g·s)
0.12
0.10
0.08
0.06
0.04
0.02
0
300
400
500
600
700
775
Temperature (K)

Figure 13

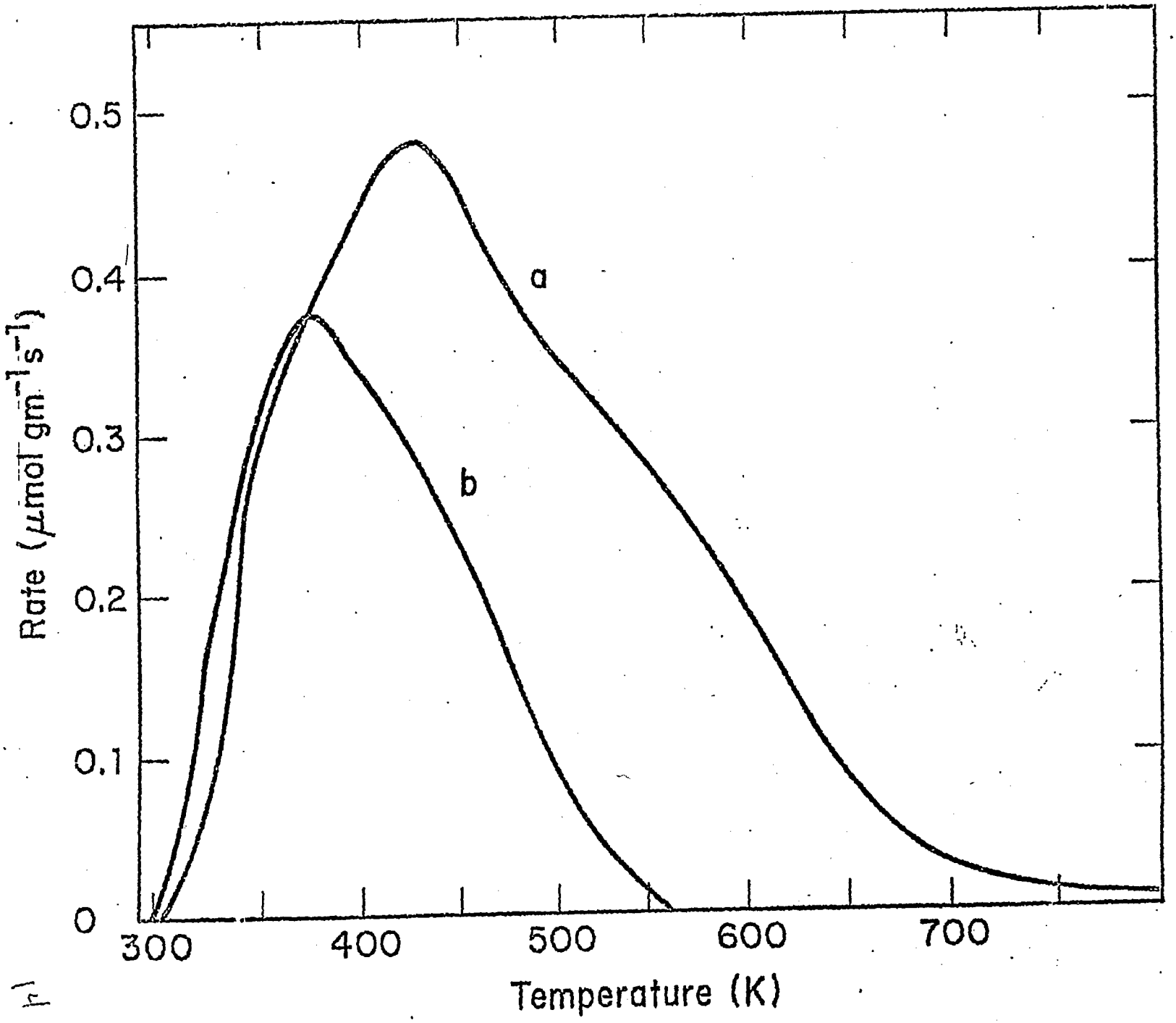
0.5
0.4
0.3
0.2
0.1
0
Rate (μmol gm^{-1}s^{-1})
a
b
300
400
500
600
700
Temperature (K)

Figure 14

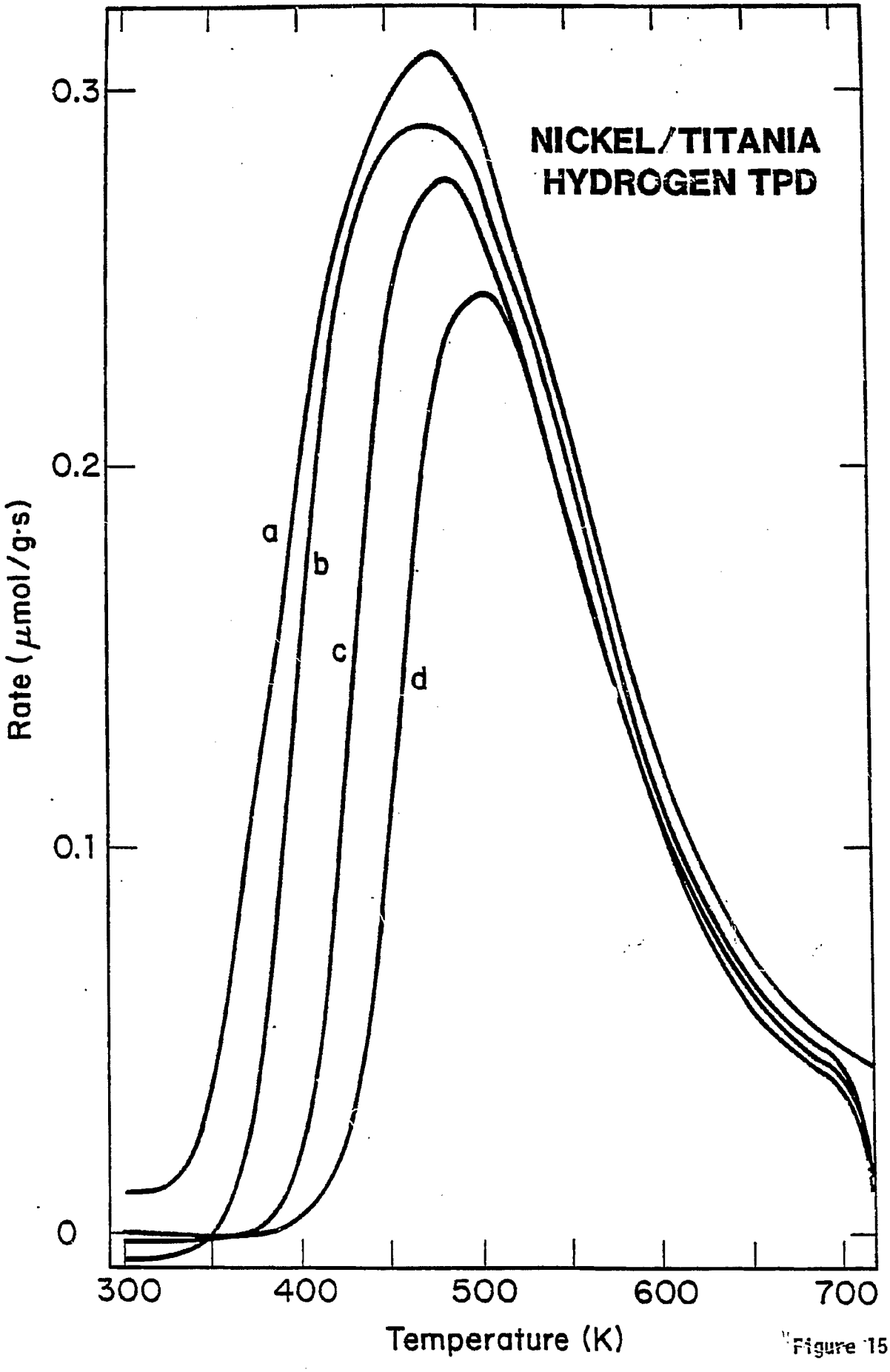
NICKEL/TITANIA
HYDROGEN TPD
Rate (μmol/g·s)
0.3
0.2
0.1
0
a
b
c
d
300
400
500
600
700
Temperature (K)

Figure 15

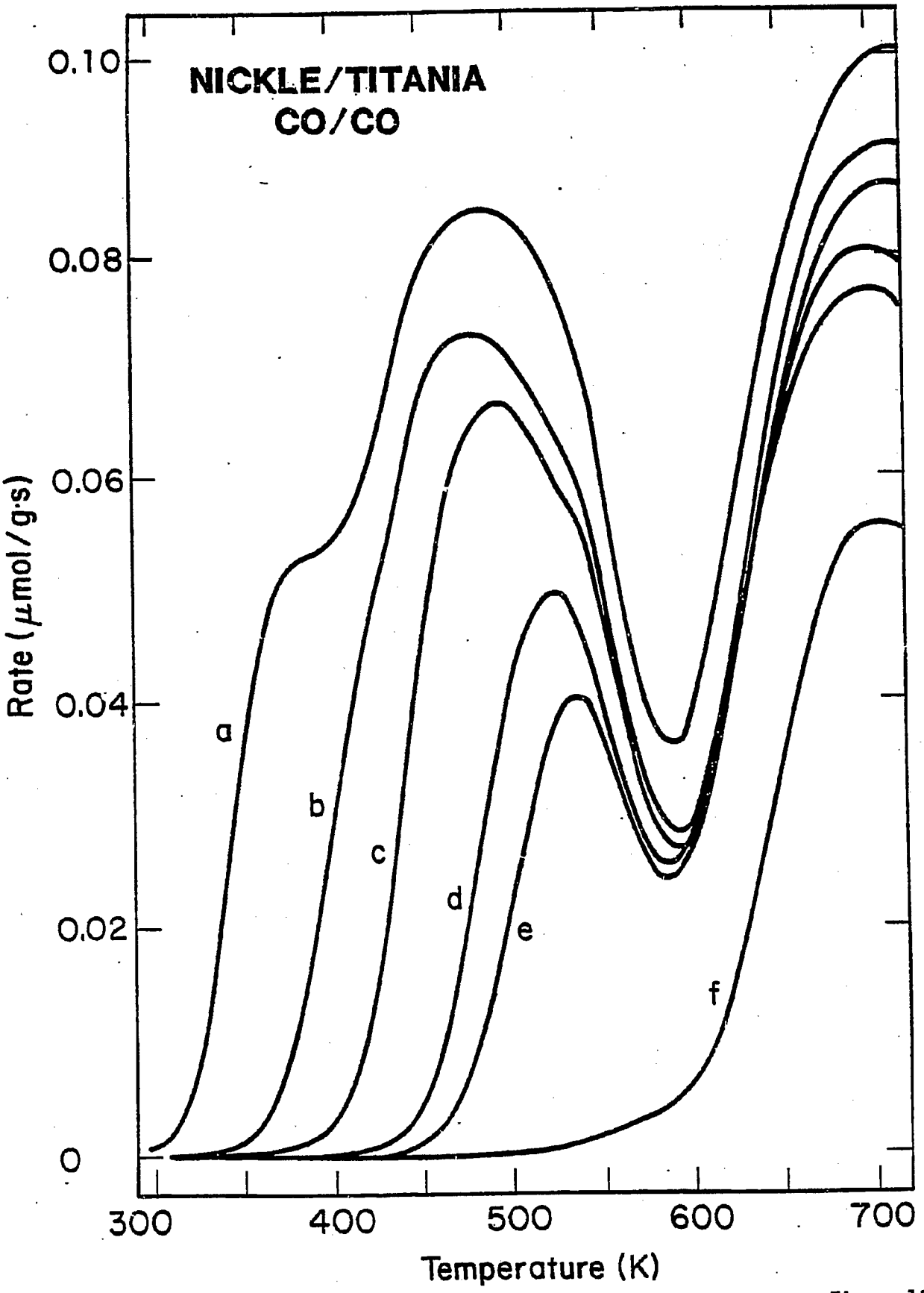
NICKLE/TITANIA
CO/CO
0.10
0.08
0.06
0.04
0.02
0
Rate (μmol/g·s)
a
b
c
d
e
f
300
400
500
600
700
Temperature (K)

Figure 16

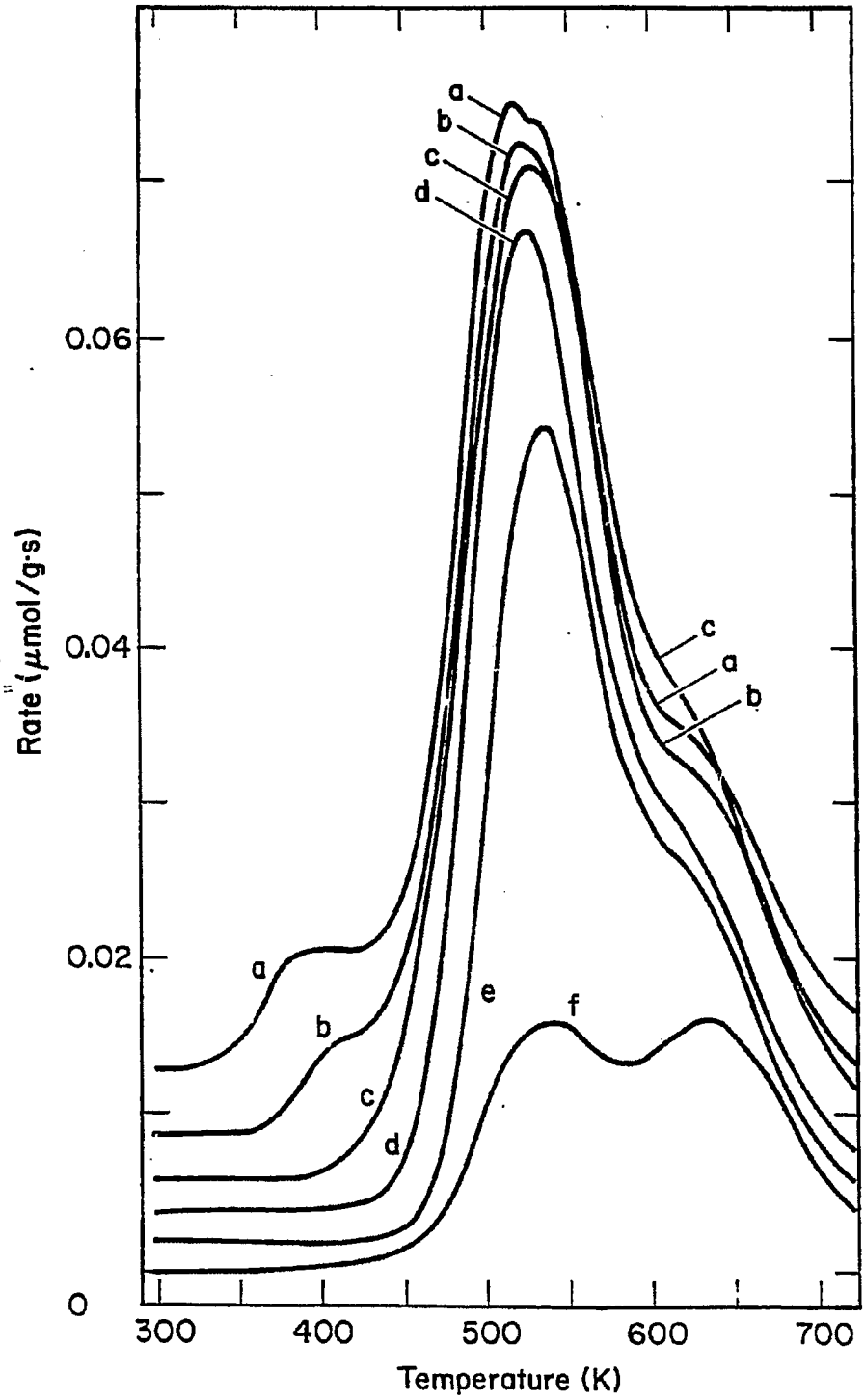
Rate (μmol/g·s)
0.06
0.04
0.02
0
300
400
500
600
700
Temperature (K)
a
b
c
d
e
f

Figure 17

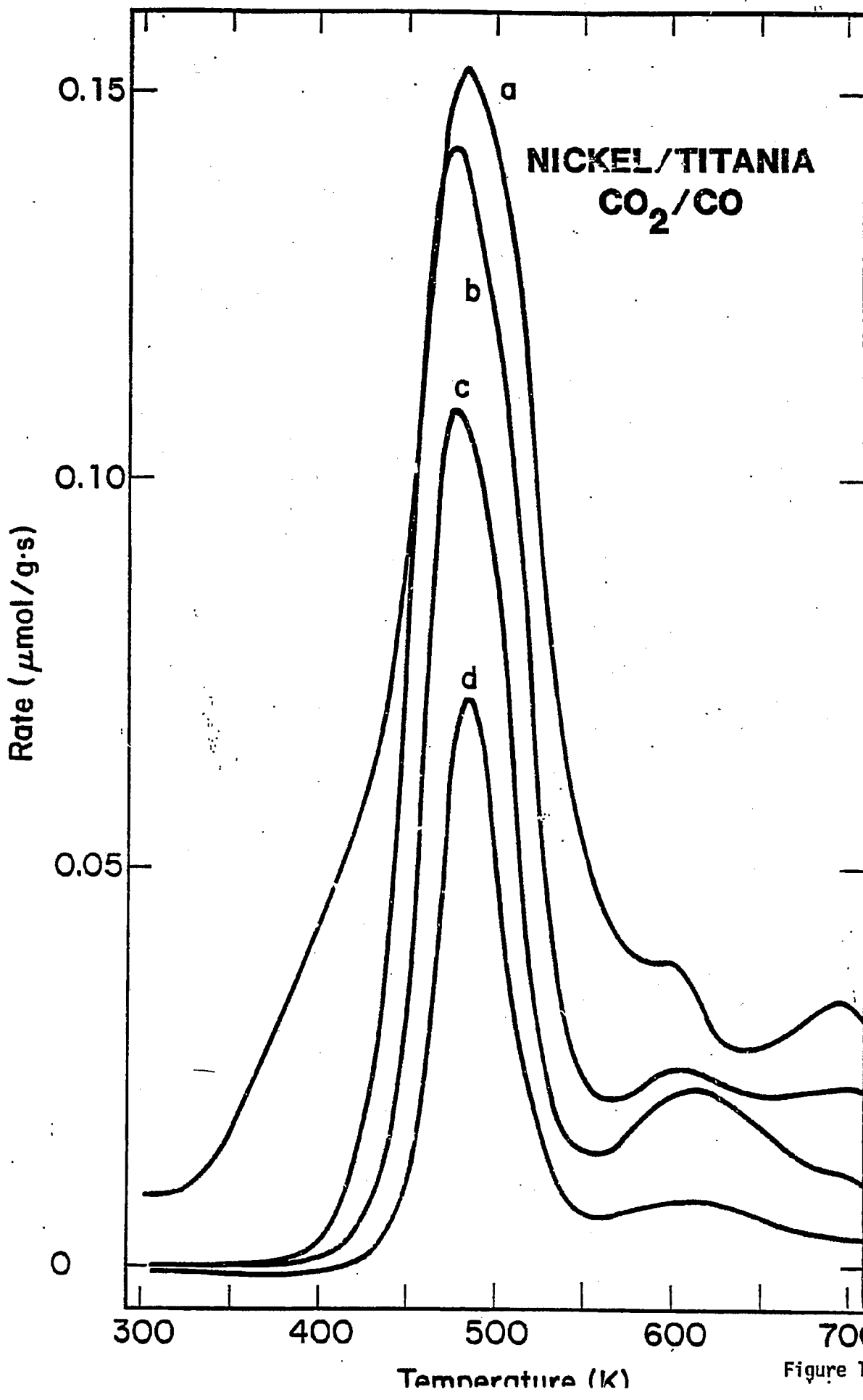
NICKEL/TITANIA
CO_2/CO
a
b
c
d
0.15
0.10
0.05
0
Rate (μmol/g·s)
300
400
500
600
700
Temperature (K)

Figure 18

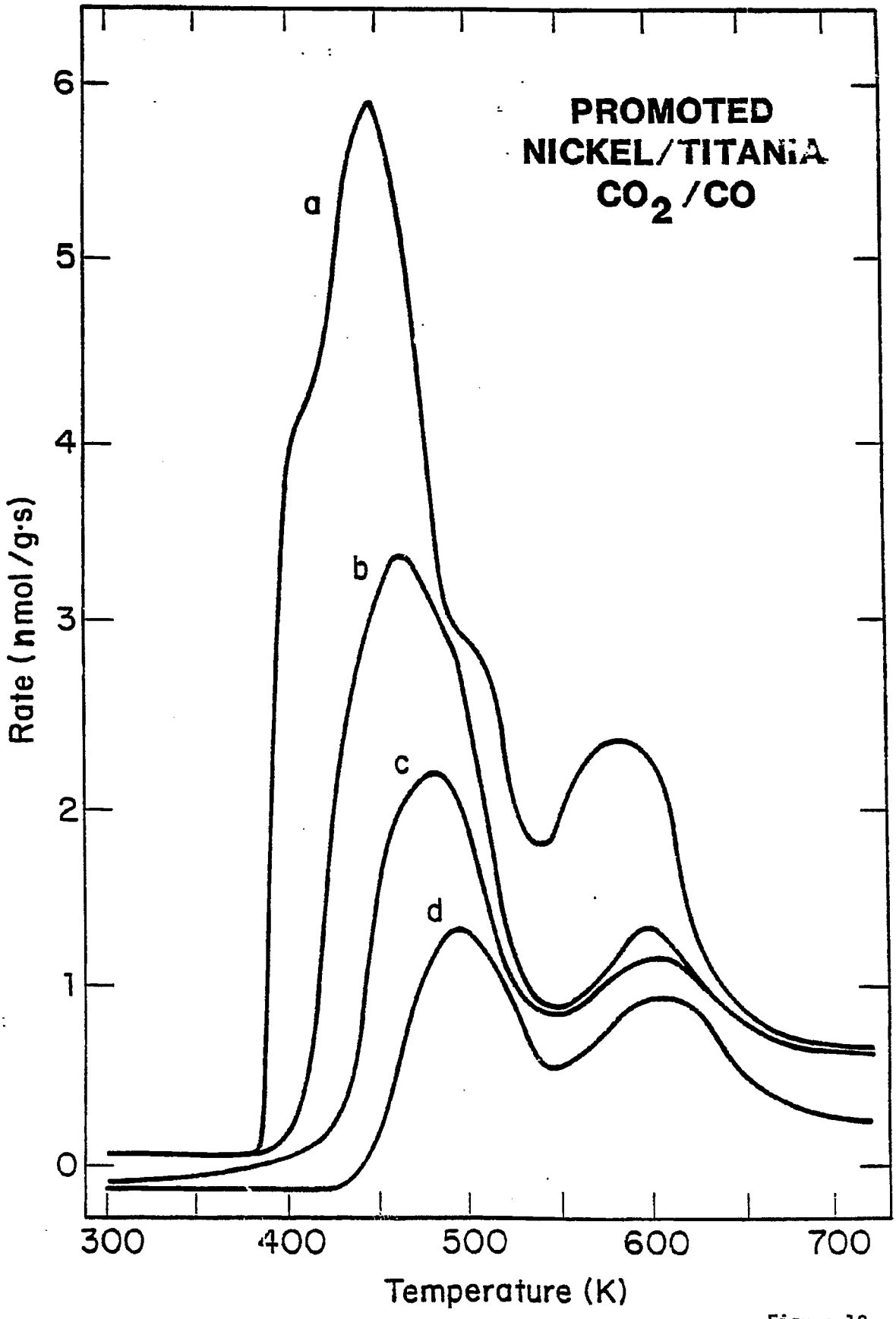
PROMOTED
NICKEL/TITANIA
CO_2 /CO
a
b
c
d
Rate (nmol/g·s)
0
1
2
3
4
5
6
300
400
500
600
700
Temperature (K)

Figure 19